


Research Article

The role of lithology and climate on bedrock river incision and terrace development along the Buffalo National River, Arkansas

Kathleen Rodrigues^{a*} , Amanda Keen-Zebert^a, Stephanie Shepherd^b, Mark R. Hudson^c, Charles J. Bitting^d, Bradley G. Johnson^e and Abigail Langston^f

^aDivision of Earth and Ecosystem Sciences, Desert Research Institute, Reno, Nevada, USA, 86512; ^bDepartment of Geoscience, Auburn University, Auburn, Alabama, USA, 36849; ^cU.S. Geological Survey, Denver, Colorado, USA, 80225; ^dNational Park Service, Buffalo National River, Harrison, Arkansas, USA, 72601; ^eEnvironmental Studies Department, Davidson College, Davidson, North Carolina, USA, 28035 and ^fDepartment of Geography and Geospatial Sciences, Kansas State University, Manhattan, Kansas, USA, 66506

Abstract

The Buffalo National River in northwest Arkansas preserves an extensive Quaternary record of fluvial bedrock incision and aggradation across lithologies of variable resistance. In this work, we apply optically stimulated luminescence (OSL) dating to strath and fill terraces along the Buffalo River to elucidate the role of lithology and climate on the development of the two youngest terrace units (Q_{tm} and Q_{ty}). Our OSL ages suggest a minimum strath planation age of ca. 250 ka for the Q_{tm} terraces followed by a ca. 200 ka record of aggradation. Q_{tm} incision likely occurred near the last glacial maximum (LGM), prior to the onset of Q_{ty} fill terrace aggradation ca. 14 ka. Our terrace ages are broadly consistent with other regional terrace records, and comparison with available paleoclimatic archives suggests that terrace aggradation and incision occurred during drier and wetter hydrological conditions, respectively. Vertical bedrock incision rates were also calculated using OSL-derived estimates of Q_{tm} strath planation and displayed statistically significant spatial variability with bedrock lithology, ranging from ~35 mm/ka in the higher resistance reaches and ~16 mm/ka in the lower resistance reaches. In combination with observations of valley width and terrace distribution, these results suggest that vertical processes outpace lateral ones in lithologic reaches with higher resistance.

Keywords: Strath terraces, Geochronology, OSL dating, Paleoclimate, Bedrock rivers, Geomorphology

(Received 7 September 2022; accepted 28 March 2023)

INTRODUCTION

Bedrock channel incision drives the topographic evolution of landscapes, often preserving geomorphic markers in the form of strath terraces that represent interruptions in continuous river-downcutting processes. Strath terrace formation requires a period of sustained lateral erosion of valley walls at a higher rate than channel bed incision, followed by a period of rapid incision that results in the abandonment of a strath surface (Gilbert, 1877; Merritts et al., 1994; Hancock and Anderson, 2002; Montgomery, 2004; Bufe et al., 2016). The formation and preservation of strath terraces often have been associated with climate change that supports variability in the ratio of transport capacity to sediment flux (Bull, 1991; Personius et al., 1993; Wegmann and Pazzaglia, 2009). Strath terraces may also form in response to base level change arising from tectonic uplift or a change in sea level (Lavé and Avouac, 2001; Van Der Woerd et al., 2001; Harkins et al., 2005), or, in some cases, in the absence of any external

forcing by way of autogenic processes (Finnegan and Dietrich, 2011; Limaye and Lamb, 2014, 2016; Scheingross et al., 2020).

It has been surmised that lithology plays a strong role in governing the rate of bedrock channel incision (Howard, 1994; Whipple and Tucker, 1999; Cook et al., 2009; Bishop and Goldrick, 2010; Forte et al., 2016), but supporting quantitative evidence for this assumption is largely lacking. In rivers with heterogeneous lithologies, variation in lithologic resistance is expected to result in variable bedrock erosion rates. Processes originating upstream (discharge and sediment supply) and downstream (base level) can affect the rate of landscape down-wearing and both upstream and downstream processes are influenced by lithologic heterogeneity across catchments. Gilbert (1877) suggested that asymmetry between the erosional resistance of the bedload and the stream bed and banks controls the distribution of lateral and vertical erosion. In more resistant reaches, vertical processes form steep canyons, and in reaches with weak lithology, where bank resistance is lower than the bedload supplied from upstream, lateral processes form wide floodplains (Gilbert, 1877). Previous studies have suggested that lateral processes are prevalent in lithologies susceptible to rapid subaerial mechanical weathering (e.g., in shales or siltstones) (Montgomery, 2004; Schanz and Montgomery, 2016; Marcotte et al., 2021). In these lithologies, valleys can widen faster than they incise vertically, leading to

*Corresponding author email address: <krodrigues@nevada.unr.edu>

Cite this article: Rodrigues K, Keen-Zebert A, Shepherd S, Hudson MR, Bitting CJ, Johnson BG, Langston A (2023). The role of lithology and climate on bedrock river incision and terrace development along the Buffalo National River, Arkansas. *Quaternary Research* 115, 179–193. <https://doi.org/10.1017/qua.2023.16>



wide, beveled bedrock surfaces. An influx of sediment that protects the bed followed by rapid incision preserves terraces in the landscape. With few exceptions, however, little work has been done to substantiate field observations of valley width and terrace preservation with geochronologic measurements across a variety of rock types, geological settings, and timescales (Wegmann and Pazzaglia, 2009; Schanz and Montgomery, 2016).

In this study, we apply optically stimulated luminescence (OSL) dating to strath and fill terraces preserved along the Buffalo National River (otherwise referred to as the Buffalo River), building upon a body of work that has shown that valley width is narrower where the river incises more resistant bedrock lithologies relative to less-resistant bedrock lithologies (Keen-Zebert et al., 2017). The OSL ages of strath terraces preserved along the Buffalo River are used to quantify rates of vertical channel incision and test the hypothesis that vertical incision rates are statistically different between bedrock lithologies. By refining the Buffalo River terrace chronology, we also seek to address questions concerning the timescales over which terraces form and

the relationship between terrace preservation and regional paleoclimate patterns.

STUDY AREA

The Buffalo River drains a $\sim 3480 \text{ km}^2$ catchment situated within the Ozark dome—a late Paleozoic uplift that developed in response to the Ouachita orogenic belt impinging from the south. Since its uplift in the Paleozoic, the Ozark dome has remained tectonically quiescent (Croneis, 1930; Hudson et al., 2011; Keen-Zebert et al., 2017; Fig. 1). The catchment is characterized by gently dipping sedimentary rocks interrupted by a succession of monoclinial folds and closely associated faults (Croneis, 1930; Hudson et al., 2011; Keen-Zebert et al., 2017; Hudson and Turner, 2022). The Buffalo River is a meandering, gravel-mantled, bedrock river that empties into the White River, which likely controls the Buffalo River's base level. The Buffalo River has spatially variable channel and valley width, flowing through wide unconfined reaches where broad floodplains form and through confined

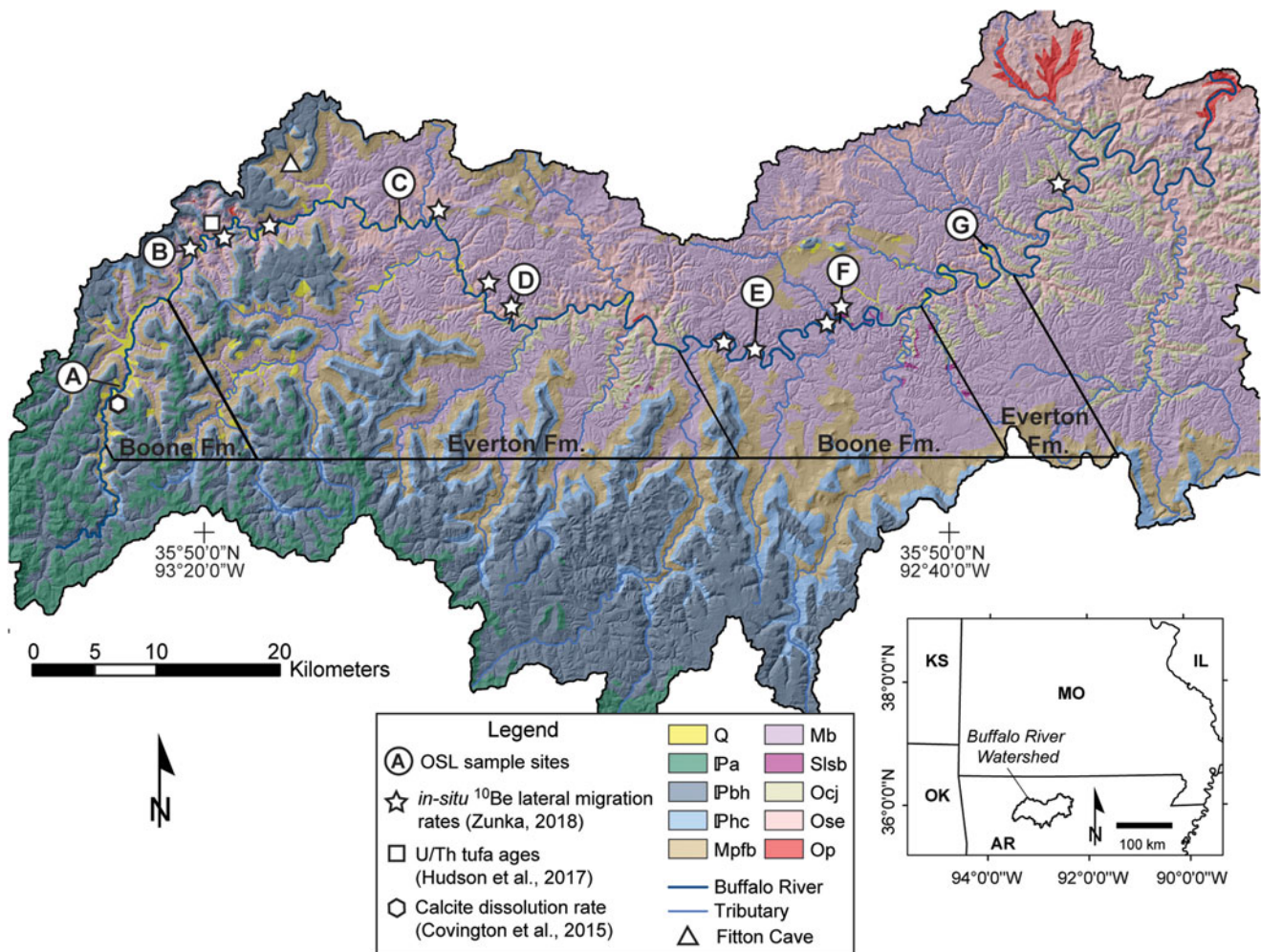


Figure 1. The Buffalo National River watershed with 5-m DEM hillshade and mapped geological units. The inset shows the location of the Buffalo River watershed in northwest Arkansas. The river flows from west to east. OSL sample locations are listed as letters: (A) Boxley; (B) Steel Creek; (C) Ozark; (D) Blue Hole; (E) Margaret White; (F) Tyler Bend; (G) South Maumee. Geological units for the Buffalo River watershed include the Quaternary deposits including the terraces studied here (Q); Pennsylvanian Atoka Formation (IPa); Pennsylvanian Bloyd Formation and Prairie Grove Member of the Hale Formation (IPbh); Pennsylvanian Cane Hill Member of Hale Formation (IPhc), Mississippian Pitkin Limestone, Fayetteville Shale, Batesville Sandstone (Mpfb), Mississippian Boone Formation (Mb), Silurian Lafferty, St. Clair, and Brassfield limestones (Slsb); Ordovician Carson Shale, Fernvale Limestone, Platin Limestone, and Kimmswick Limestone, and Joachim Dolomite (Ocj); Ordovician St. Peter Sandstone and Everton Formation (Ose); and Ordovician Powell Dolomite (Op). Refer to Keen-Zebert et al. (2017) and references therein for complete lithologic descriptions. Figure adapted from Zunka (2018).

narrower reaches where the channel flow is laterally restricted, and floodplains form only on the inside of ingrown meander bends that are cut into bluffs that are as tall as 168 m.

The Buffalo River cuts through Ordovician, Mississippian, and Pennsylvanian carbonate and clastic sedimentary rocks that are subject to both physical and chemical (karstic) weathering (Keen-Zebert et al., 2017; Fig. 2A). There are four main lithologic reaches in the Buffalo River made up of two dominant lithologies: the Boone and Everton Formations. The upstream reach of the main stem of the Buffalo River is incised into the Boone Formation limestone and characterized by wide valleys. Farther downstream at approximately river km 30, the channel incises the Everton Formation sandstone and the valley narrows. At river km 114, faulting has returned the Boone Formation to the surface and the pattern is repeated; the valley widens just

downstream of the contact with the Boone Formation and then narrows where down-cutting has exposed the Everton Formation to the surface (Keen-Zebert et al., 2017; Fig. 2B).

The Boone Formation consists of limestone with interbedded chert. Where the channel occupies the Boone Formation, fluvio-karst processes and factors, including the elevation of the water table, chemical weathering, dissolution of the channel bed, and ground water-surface water interaction, play a large role in channel incision (Anthony and Granger, 2007). Evidence of phased incision is preserved in fluvial terraces and in a series of horizontal cave passages that are now perched above the water table. Where the channel occupies the Boone Formation, it meanders across a wide continuous floodplain and is characterized by a bedrock-floored channel with a boulder, cobble, coarse gravel, and sand bedload that is deposited in point and lateral bars.

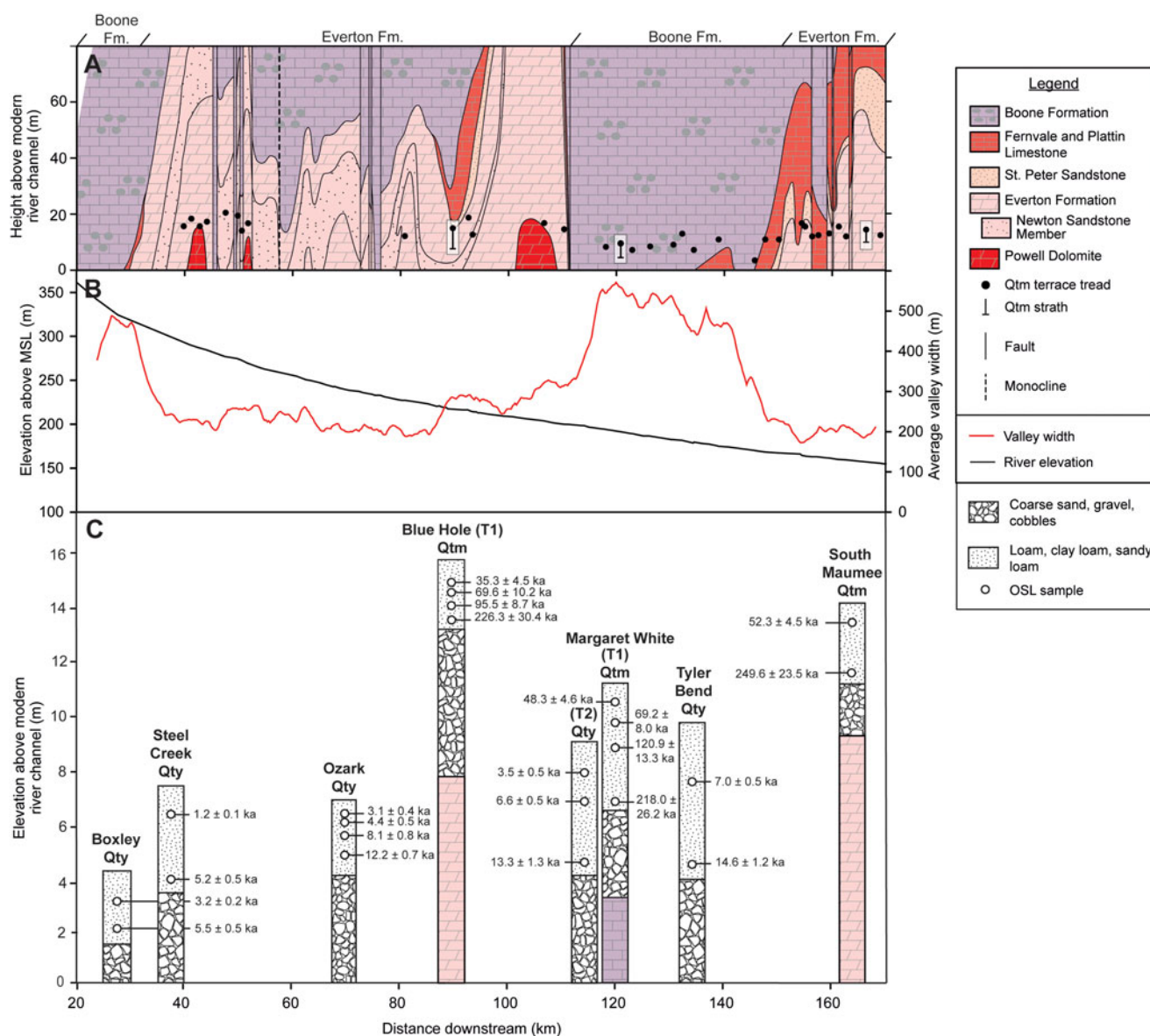


Figure 2. (A) Changes in valley lithology and Qtm strath terrace tread elevations over downstream distance. Lithological reaches are subdivided based on the lithology exposed at modern river level. Qtm terraces dated in this study are highlighted in white boxes; circles correspond to their tread elevations; dashes (within the white boxes) refer to their buried straths. (B) Buffalo River longitudinal profile and valley width over downstream distance; MSL = mean sea level. (C) Simplified stratigraphic columns from each sampled Qty and Qtm terrace showing OSL ages and major changes in sedimentology with depth. (A) and (B) are adapted from Keen-Zebert et al. (2017).

The Everton Formation, which underlies the Boone Formation, is composed of interbedded dolostone, limestone, and sandstone. The middle part of the Everton is dominated in the upper reaches (upstream of river km ~75) by a thick sandstone sequence known as the Newton Sandstone Member, which thins significantly toward the lower reaches (Fig. 2A; Keen-Zebert *et al.*, 2017). There is less ground water-surface water interaction in the Everton Formation than in the Boone Formation, and thus the effect of fluvio-karst processes is reduced. The Boone and Everton Formations have statistically equivalent mechanical resistance, but the Everton Formation has significantly higher chemical resistance owing to both its higher content of insoluble material and the lower dissolution rate of dolomite versus limestone (Keen-Zebert *et al.*, 2017). Where the channel occupies the Everton Formation, it is characteristic of ingrown meandering bedrock channels with a bedrock channel bed, high bedrock bluffs on the outsides of meanders, with high amplitude, narrow valleys, and floodplains formed on the insides of meanders. The contrasting valley characteristics have been taken to suggest that vertical channel processes are more prevalent in the Everton Formation reaches relative to the Boone Formation reaches (Keen-Zebert *et al.*, 2017).

Geomorphic evidence of phased incision is preserved in both the Boone and Everton Formation reaches of the river. Geologic mapping (1:24,000) of the Buffalo River conducted by the United States Geological Survey and the Arkansas Geological Survey (see references in Keen-Zebert *et al.*, 2017) documents flights of successive, stepped, terraces adjacent to the river, which are designated as Qty (young), Qtm (medial), and Qto (old) based on their elevation above the modern channel. Qty denotes Holocene fill terraces with treads <12 m above the modern channel. Qty terraces preserve basal coarse gravel and boulders and are overlain by ~3–9 m of finer-grained sediments typically dominated by sand. Qtm indicates strath terraces capped by alluvial sediments ~5–10 m thick that include coarse channel-lag deposits at their base and are covered by a drape of overbank deposits dominated by sand. The Qtm terrace treads occur at ~12–16 m above the modern channel with elevations that are higher in the Everton Formation reaches relative to the Boone Formation reaches (ANOVA *p*-value <0.00001; Fig. 2A). The terraces indicated by Qto are very poorly preserved strath terraces ~16–90 m above the modern channel that are overlain by a thin veneer of sandy soil interspersed with gravel and cobbles. OSL dating of the Qto terrace deposits is hampered by the poor preservation and highly disturbed nature of the deposits. The fluvial sediments capping the Qtm and Qty terraces archive the aggradation and incision history of the Buffalo River over the late Quaternary and are the focus of this paper.

The modern climate of the Buffalo River watershed is temperate continental and characterized by long summers and short, relatively mild winters (Mott and Luraas, 2004). The average annual precipitation is ~117 cm with drier months in the summer and wetter months in the spring and fall. Occasional flooding occurs throughout the year with major events occurring more commonly after the dry season (Mott and Luraas, 2004).

METHODS

Field observations and sample collection

The elevations of previously mapped Qtm terraces were measured from a 1-m digital elevation model (DEM) acquired from the Buffalo River National Park Service. Mean tread elevations for

all mapped Qtm terraces are shown in Figure 2A. Cross-sectional profiles for each of the three Qtm terraces selected in this study also were extracted from the 1-m DEM (Fig. 3). At Blue Hole, the subsurface stratigraphy was mapped at high resolution using boreholes drilled at horizontal intervals of ~20 m. At Margaret White and South Maumee, the subsurface stratigraphy was projected from exposures observed in the trenches and auger holes where OSL samples were collected, and from outcrops observable from the modern floodplain. The Qty fill terraces were similarly described in the field from trenches, auger holes, and bank exposures.

To evaluate differences in terrace ages, timescales of terrace occupation, and incision rates across the Buffalo River, three Qtm and five Qty terraces were selected for OSL dating. OSL samples were collected by hammering stainless steel tubes horizontally into freshly cleaned trench faces or in some cases by vertical hand-augering (Fig. 4). The sampling strategy was designed to place chronological controls on the onset of aggradation and terrace abandonment by collecting samples from close to the strath unconformity and top of each terrace deposit. At some study sites, a higher density of samples was collected to evaluate possible changes in the rate of terrace aggradation. To assess the extent of partial bleaching in our ancient terrace samples, two modern samples also were collected from the modern floodplain: one sample from recent flood deposits on top of the floodplain (BR005) and the other sample from the floodplain bank, ~1.5 m below the surface of the top of the floodplain (BR002). In all cases, care was taken to ensure that samples were collected where alluvial sediment appeared to be *in situ* and not reworked by anthropogenic and/or hillslope processes.

OSL dating

Sample preparation

Preparation and analysis of OSL samples was carried out at the Desert Research Institute Luminescence Laboratory (DRILL) in Reno, Nevada, under dim orange light. Sample tubes were opened and the sediment at either end of the tube was removed to prevent contamination of the working sample with light-exposed grains. Standard coarse-grain quartz preparation was carried out using methods described in Aitken (1998). This included a 10% HCl and 30% H₂O₂ treatment to remove carbonates and organic material, respectively. Wet sieve methods were used to obtain the 180–250 μm grain size fraction and a heavy liquid separation using lithium heteropolytungstate (LST) was performed to isolate the quartz fraction. The remaining quartz grains were treated with 40% HF for 40 minutes to etch the alpha-irradiated surface of the quartz and remove any remaining feldspar from the samples.

Representative subsamples (~30 g) of dose rate sediment were analyzed for radioelemental concentrations of U, Th, and K using inductively coupled plasma-mass spectrometry (ICP-MS) and inductively coupled plasma-atomic emission spectrometry (ICP-AES) analyses at the ALS Geochemistry Facility in Reno, Nevada. Moisture content was measured for all samples. Dose rate calculations incorporated dose rate conversion factors from Guérin *et al.* (2011) and Liritzis *et al.* (2013), estimated moisture content over the burial period, and cosmic dose contribution following Prescott and Hutton (1994). All annual dose rates include an internal alpha and beta contribution of 10.5 μGy/a (Rink and Odom, 1991).

Equivalent dose determination and age calculation

Single grain measurements were made using aluminum discs that contain 100 holes (each hole 300 μm in diameter and 300 μm in

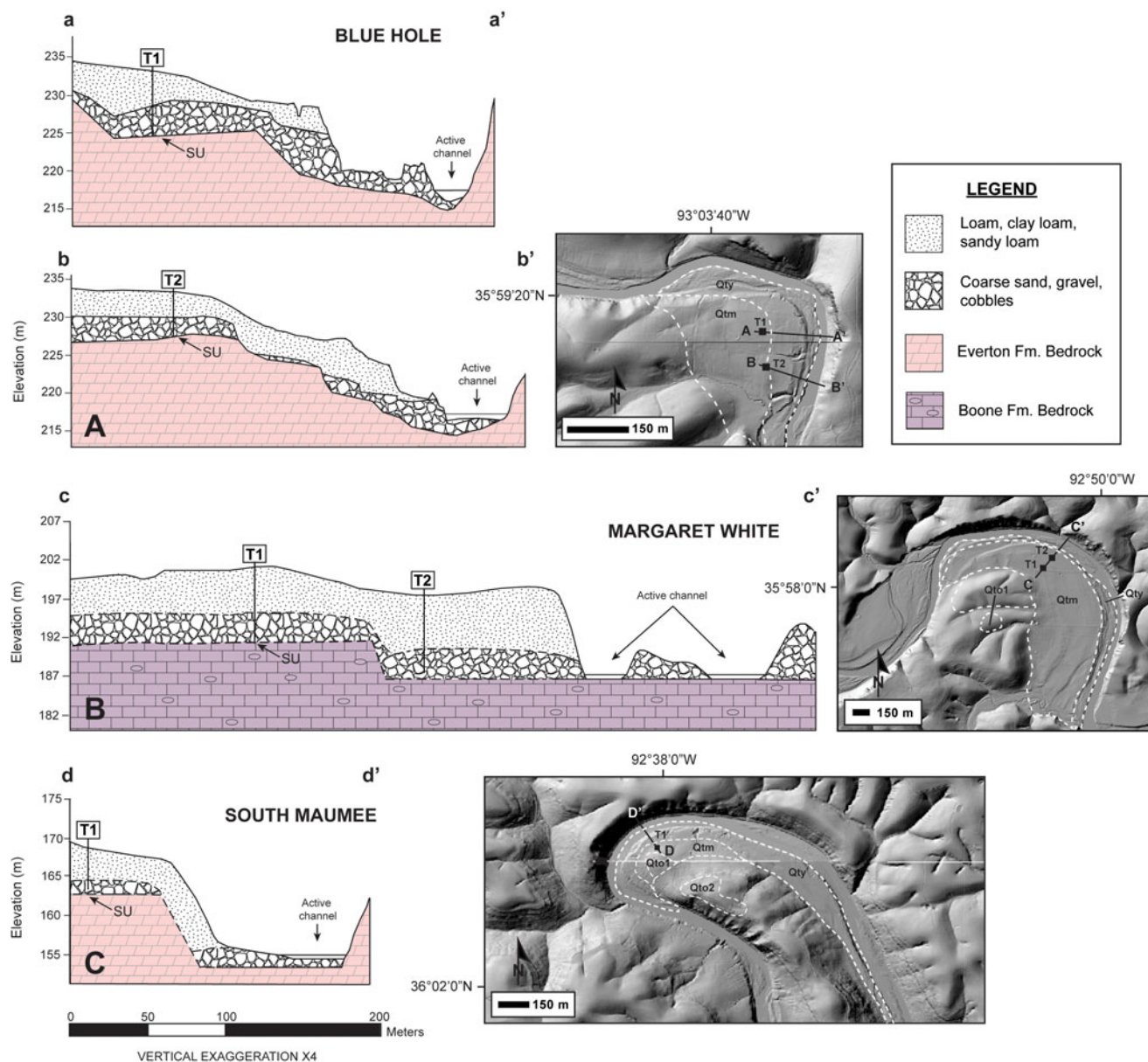


Figure 3. (A–C) Cross-sectional profiles of the three Qtm terrace study sites with mapped lithological contacts. Trenches where OSL samples were collected are labeled with a ‘T#’ corresponding to the data in Table 1. Dashed lines represent uncertainty in the position of lithological contacts. ‘SU’ refers to the strath unconformity used for vertical incision rate calculations. Inset figures show profile orientation on LiDAR images and sample numbers for each site. The mapped terrace boundaries refer to those provided in the geologic maps of Chandler and Ausbrooks (2015a, b) and Turner and Hudson (2010).

depth) arranged in a 10×10 grid. To ensure that only one grain occupied an individual hole, each disc was visually checked under a light microscope prior to measurement. Luminescence measurements were performed using an automated Risø TL-DA-20 luminescence reader using a focused green (532 nm) laser for stimulation ($\sim 45 \text{ mW/cm}^2$) and detection through a 7-mm-thick Hoya U-340 UV transmitting filter. Laboratory irradiations were performed using a calibrated $^{90}\text{Sr}/^{90}\text{Y}$ beta radioactive source attached to the Risø luminescence reader and delivering $\sim 0.13 \text{ Gy/s}$. OSL signals were measured after a one second period of stimulation, with the OSL signal being integrated from the first 0.06 s of the decay curve, and the subtracted background from the last 0.2 s. Equivalent dose measurements followed the SAR protocol with an embedded IR depletion test (Murray and

Wintle, 2000, 2003; Duller, 2003). Dose recovery tests (Murray and Wintle, 2003) applying different preheat temperatures (ranging from 160–280°C) were performed on 21 aliquots of sample BUFF036 in order to test the reliability of the SAR protocol and determine the optimal preheat temperature for single grain OSL measurement.

Owing to early signal saturation, the conventional OSL dating limit was reached at ages of ca. 125 ka. Feldspars, which typically saturate at higher D_e values, were effectively absent in the samples studied, and therefore a thermally transferred OSL (TT-OSL) SAR protocol following the methodology of Porat et al. (2009) was applied to the remaining older terrace deposits. Because TT-OSL signals saturate at much higher doses relative to conventional OSL, the dating range typically can be extended by a factor

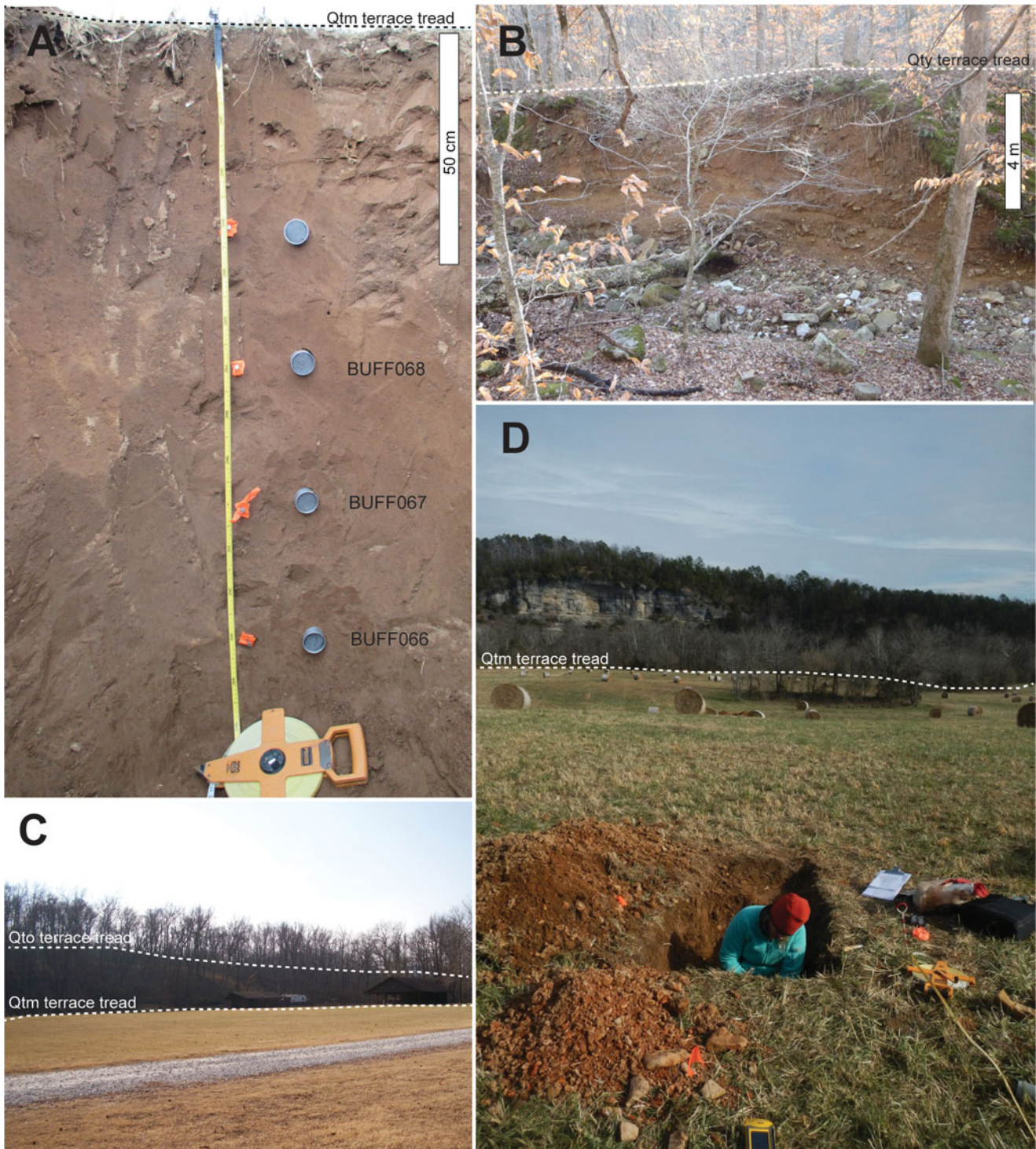


Figure 4. Field photos showing typical features of Qtm and Qty terraces preserved along the Buffalo River. (A) Margaret White Qty T2 terrace with OSL samples hammered into the trench wall; note the stratigraphic homogeneity, which is typical for the Buffalo River terrace deposits. (B) Boxley Qty terrace shown in profile from the perspective of the modern channel. (C) Qtm and Qto terraces preserved at Ozark. (D) Blue Hole Qtm T1 location with tall bluffs exposed in the background opposite the Buffalo River.

of 2–3 (e.g., Wang *et al.*, 2006). Our TT-OSL measurements were carried out on 7 mm multigrain quartz aliquots (~650 grains) using the same Risø TL-DA-20 luminescence reader with blue LED stimulation (~45 mW/cm²). The ⁹⁰Sr/⁹⁰Y beta radioactive source delivered a calibrated dose rate of ~0.11 Gy/s to the

stainless-steel discs used for TT-OSL analysis. The effectiveness of this TT-OSL protocol was tested using a dose recovery test on 20 aliquots of sample BUFF044. A residual dose of 28 ± 8 Gy (determined from the TT-OSL Central Age Model [CAM] [Galbraith *et al.*, 1999] D_e from modern sample BR002), was subtracted from

Table 1. OSL ages and inferred vertical bedrock incision rates for three Qtm terraces on different lithologically defined reaches of the Buffalo River. Vertical bedrock incision rates were calculated based on the OSL-derived ages from nearest the strath unconformity and the elevation of the underlying bedrock surface above the modern channel. Data in bold were used to calculate bedrock incision rates at each site. For a compilation of all data used for dose rate and age calculation see Supplementary Table 4.

Location	Bedrock lithology	Sample number	Sample depth (m)	Equivalent Dose (Gy) ¹	Total dose rate (Gy/ka) ²	Age (ka)	Qtm Strath height above the modern channel (m)	Vertical bedrock incision rate (mm/ka)	
Blue Hole T1	Upper part of Everton Fm. (Oeu)	BUFF035	0.8	85.8 ± 7.8	1.9 ± 0.1	35.3 ± 4.5	8.0		
		BUFF036	1.1	126.2 ± 17.0	1.8 ± 0.1	69.6 ± 10.2			
		BUFF026	1.4	166.3 ± 11.8	1.7 ± 0.1	95.5 ± 8.7			
		BUFF025	2.2	*397.3 ± 48.2	1.8 ± 0.1	226.3 ± 30.4			35.4 ± 6.8
		BUFF039	0.4	95.4 ± 16.4	1.6 ± 0.1	57.8 ± 10.5			
Blue Hole T2		BUFF040	0.7	138.5 ± 27.3	1.6 ± 0.1	85.0 ± 17.5	8.5		
		BUFF044	1.3	*402.3 ± 42.6	1.7 ± 0.1	242.7 ± 29.1			35.0 ± 6.1
		BUFF064	0.5	100.1 ± 10.1	2.1 ± 0.1	48.3 ± 5.6			
Margaret White T1	Boone Fm. (Mb)	BUFF063	1.0	149.0 ± 14.9	2.2 ± 0.1	69.2 ± 8.0	3.5		
		BUFF062	1.3	*239.2 ± 22.4	2.0 ± 0.1	120.9 ± 13.3			
		BUFF061	3.8	*344.1 ± 36.1	1.6 ± 0.1	218.0 ± 26.2			16.1 ± 4.2
		BUFF080	0.9	47.1 ± 3.5	0.9 ± 0.1	52.3 ± 4.5			
South Maumee	Upper part of Everton Fm. (Oeu)	BUFF081	3.7	*241.1 ± 18.3	1.0 ± 0.1	249.6 ± 23.5	9.0	36.1 ± 5.4	

¹Equivalent doses were calculated using the Average Dose Model (Guérin et al., 2017) and incorporate a σ_m of 0.12.

²External dose rates are based on U, Th, and K_2O measured by ICP-MS and ICP-AES. Dose rates were calculated using the conversion factors of Liritzis et al. (2013) and are shown rounded to one decimal place; ages were calculated using values prior to rounding. Dose rates were calculated assuming a water content of $10 \pm 6\%$. External dose rates also include a cosmic dose component calculated according to Prescott and Hutton (1994). Total dose rates include an internal dose rate of 0.011 ± 0.001 Gy/ka, which was calculated based on assumed internal U and Th concentrations provided by Rink and Odom (1991).

*Equivalent doses were determined using a TT-OSL protocol on multigrain aliquots and incorporate a 28 ± 8 Gy residual subtraction.

all TT-OSL D_e values prior to age calculation (refer to Supplementary Tables 1 and 2 for details about the measurement protocols used in this study).

All measurements were required to pass the following criteria for further analysis: <20% test dose error, <20% recycling ratio error, <5% recuperation, <20% equivalent dose error, and a signal $>3\sigma$ above background. D_e values also were rejected if they were $>2D_0$, following the recommendations of Wintle and Murray (2006). All individual D_e values incorporate an instrumental error of 1.5%.

RESULTS

Terrace characteristics

Terrace elevations and general sediment characteristics are provided in Figure 2C. The three Qtm terraces selected for this study preserved morphologically similar alluvial deposits, with bedrock straths capped by a layer of coarse-grained sand, gravel, and cobbles ranging from ~2–4 m in thickness and immediately overlain by 2–4 m of loamy overbank deposits lacking any prominent stratigraphic features (Fig. 4A). The Qtm terrace treads were generally planar with the exception of Blue Hole, which featured dipping alluvium cover overlying a series of minor ‘complex-response’ strath terraces (sensu Bull, 1990). The provenance for the cobbles and gravels overlying the straths at all sites had mixed non-local lithologies compared to the local bedrock lithology, confirming that the clasts were transported by fluvial rather than by hillslope processes. The Qty terraces similarly preserved ~1–4 m of basal cobbles and gravels and were overlain by

2–4 m thick loam deposits dominated by sand (Fig. 4B). Evidence for natural or anthropogenic sediment mixing or hillslope processes was isolated to the upper 40–70 cm of the deposits.

Single grain OSL characteristics

Preliminary OSL testing showed that samples consistently reproduced a given dose using the SAR protocol, yielding an average dose recovery ratio of 0.97 ± 0.08 ($n = 21$). Thermal transfer tests showed no significant evidence for thermal transfer over the range of preheat temperatures tested (<0.1 Gy). Quartz OSL signals were typically bright and dominated by the fast component (Fig. 5A). Growth curves were best described by the sum of two saturating exponential functions with D_0 values for the early saturating component ranging from ~9–20 Gy and the slowly saturating component ranging from ~74–450 Gy (Figure 5A). Sensitivity changes monitored by administering a small test dose (~6.5 Gy) after each regenerative dose showed little (<20%) change over the course of the SAR cycle. Mean recuperation and recycling ratios of $1.4 \pm 2.2\%$ and 1.04 ± 0.03 , respectively, further support the appropriateness of the SAR protocol applied to these samples.

Both modern floodplain samples (BR002 and BR005) carried no significant residual OSL signal (~0.2 Gy; Fig. 5B; Supplementary Table 1) suggesting that bleaching of the quartz OSL signal is sufficient for the fluvial sediments studied along the Buffalo River. In contrast, single grain D_e distributions for the majority of ancient samples were positively skewed and displayed overdispersion of >20% (Fig. 5C;

Table 2. OSL ages for Qty terraces. For a compilation of all data used for dose rate and age calculation see Supplementary Table 5.

Location	Sample number	Sample depth (m)	Equivalent Dose (Gy) ¹	Total dose rate (Gy/ka) ²	Age (ka)
Boxley	BUFF060	1.5	5.6 ± 0.3	1.7 ± 0.1	3.2 ± 0.2
	BUFF059	2.2	10.4 ± 0.7	1.9 ± 0.1	5.5 ± 0.5
Steel Creek	BUFF082	1.6	2.4 ± 0.2	2.0 ± 0.1	1.2 ± 0.1
	BUFF083	3.4	9.8 ± 1.0	1.9 ± 0.1	5.2 ± 0.5
Ozark	BUFF073	0.5	4.3 ± 0.5	1.4 ± 0.1	3.1 ± 0.4
	BUFF072	0.7	6.0 ± 0.6	1.4 ± 0.1	4.4 ± 0.5
	BUFF071	1.0	12.7 ± 1.0	1.6 ± 0.1	8.1 ± 0.8
	BUFF070	1.4	20.5 ± 0.8	1.7 ± 0.1	12.2 ± 0.7
Margaret White T2	BUFF068	0.7	5.0 ± 0.6	1.4 ± 0.1	3.5 ± 0.5
	BUFF067	1.0	9.9 ± 0.6	1.5 ± 0.1	6.6 ± 0.5
	BUFF066	1.3	21.2 ± 1.9	1.6 ± 0.1	13.3 ± 1.3
Tyler Bend	BUFF077	1.1	11.4 ± 0.6	1.6 ± 0.1	7.0 ± 0.5
	BUFF078	2.5	27.2 ± 1.9	1.9 ± 0.1	14.6 ± 1.2

¹Equivalent doses were calculated using the Average Dose Model (Guérin et al., 2017) and incorporate a σ_m of 0.12.

²External dose rates are based on U, Th, and K₂O measured by ICP-MS and ICP-AES. Dose rates were calculated using the conversion factors of Liritzis et al. (2013) and are shown rounded to one decimal place; ages were calculated using values prior to rounding. Dose rates were calculated assuming a water content of 10 ± 6%. External dose rates also include a cosmic dose component calculated according to Prescott and Hutton (1994). Total dose rates include an internal dose rate of 0.011 ± 0.001 Gy/ka, which was calculated based on assumed internal U and Th concentrations provided by Rink and Odom (1991).

Supplementary Table 3). Given that modern fluvial samples are expected to reflect worst-case bleaching scenarios owing to poor preservation potential (Jain et al., 2004), we suggest that the high overdispersion present in our ancient samples can be explained by some other unidentified external source of scatter (e.g., post-depositional mixing, beta microdosimetry, etc.). Most workers recommend against using the minimum age model (which is commonly applied to fluvial deposits; Galbraith et al., 1999) in scenarios where either post-depositional mixing or beta microdosimetry are the dominant influencers on overdispersed D_e distributions (Galbraith et al., 1999; Olley et al., 2004; Bateman et al., 2007). We apply the Average Dose Model (ADM, Guérin et al., 2017), which is likely better suited to isolate the D_e mode in these scenarios (Guérin et al., 2017).

Multi-grain TT-OSL characteristics

TT-OSL dose response curves exhibited single saturating exponential behavior with D_0 values ranging from 420–800 Gy (Fig. 5D). Dose recovery experiments on sample BUFF044 yielded a mean ratio of 0.95 ± 0.10 ($n = 10$), suggesting that the protocol was suitable for D_e determination. Relative to single grain measurements, TT-OSL D_e values from modern sample BR002 exhibited high overdispersion with D_e values ranging from ~0–106 Gy. The CAM TT-OSL D_e of 28 ± 8 Gy from modern sample BR002 was subtracted from each individual TT-OSL D_e prior to age calculation to account for the average residual signal that we observe. The residual-corrected TT-OSL ages from samples collected near the strath unconformity should be interpreted as minimum ages for strath planation.

OSL ages

Our OSL ages from sand collected near the Qtm strath surface at each of the three study sites suggest a minimum age of ca. 250 ka

for the onset of strath planation and aggradation (Table 1). These basal ages were statistically indistinguishable within the reported uncertainties across the three study sites. All other samples collected from the Qtm terrace fill yielded depositional ages consistent with stratigraphic position, and in all cases span an order of magnitude. Vertical incision rates calculated using ages from nearest the Qtm strath surface and strath elevation above the modern channel range from ~16 mm/ka at our Boone Formation site, Margaret White, to ~35 mm/ka at our two Everton Formation sites.

OSL ages from the Qty terraces display a younging trend upstream, with the onset of Qty aggradation beginning ca. 14.5 ka at our farthest downstream Qty terrace site, Tyler Bend, and ca. 5.5 ka at our farthest upstream site, Boxley (Table 2). The depositional ages from each terrace are in stratigraphic order, with a range that in some cases spans nearly 10 ka for a given deposit (Table 2).

DISCUSSION

OSL and TT-OSL signal characteristics

TT-OSL signals are known to be significantly less sensitive to light exposure relative to conventional OSL signals, and commonly yield age overestimates for fluvial sediments (Duller and Wintle, 2012). TT-OSL signals from well-bleached aeolian deposits typically carry residual doses that range from 5–20 Gy and from 40–380 Gy for fluvial sediments (Hu et al., 2010; Demuro et al., 2015). Based on the presence of significant residual signals, many practitioners have suggested that TT-OSL protocols should be applied only to well-bleached aeolian or shallow marine deposits (Duller and Wintle, 2012). Our OSL results from modern analogue samples suggest that contrary to many fluvial deposits, both the OSL and TT-OSL signals from Buffalo River quartz were relatively well bleached at deposition. TT-OSL results from our modern analogue sample carries an average weighted TT-OSL residual D_e of 28 ± 8 Gy (constituting 6–11% of the measured D_e), which

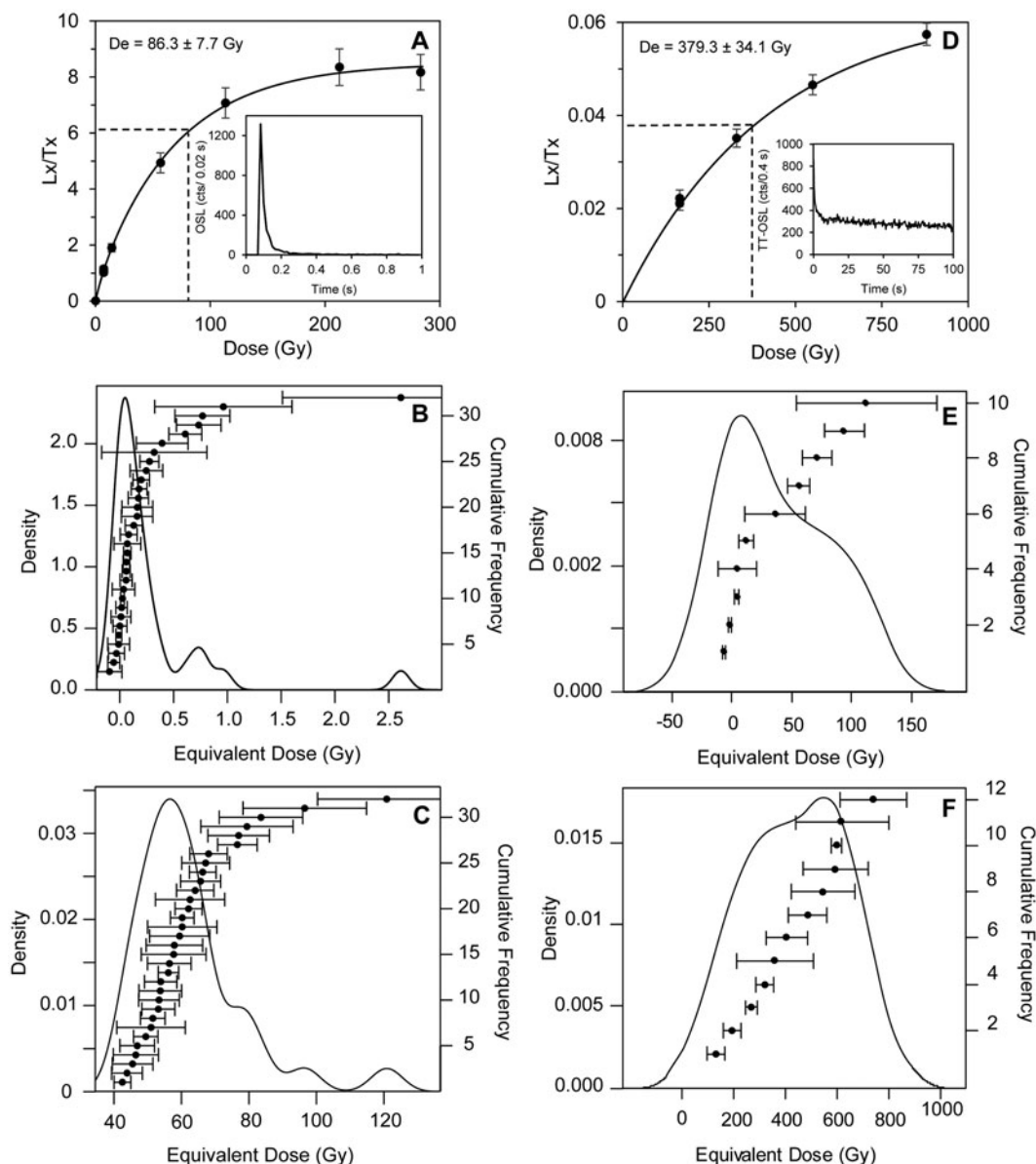


Figure 5. Luminescence characteristics of Buffalo River quartz. (A) Representative dose response curve with inset decay curve for a single grain of BUFF035 quartz; (B) equivalent dose distribution for modern sample BR002 (see Supplementary Fig. 4 for D_e distribution from the additional modern sample, BR005); (C) single grain D_e distribution for sample BUFF035; (D) TT-OSL dose response curve with inset decay curve for a multigrain quartz aliquot of BUFF044; (E) TT-OSL D_e distribution for modern sample BR002; (F) TT-OSL D_e distribution for sample BUFF044.

is comparable to published residual doses from aeolian deposits. By subtracting this residual dose from our D_e estimates, we assume that bleaching conditions of the present are representative of those that existed in the past. However, the amount of sediment present in the water column (and thus the opacity and sediment-bleaching rate) was likely different during strath planation when the river was a net-aggradational system relative to its present-day net-incisional state. In spite of this uncertainty, with subtraction of a residual dose, our TT-OSL age estimates for strath planation are indistinguishable among the three Qtm terraces studied, suggesting that residual subtraction based on a modern analogue may be appropriate in this particular fluvial setting. Further work using natural and laboratory flume experiments would be helpful to understand how varying fluvial regimes (e.g., streamflow and sediment supply) influences luminescence bleachability.

A growing body of literature has documented apparent age underestimation of the TT-OSL signal relative to other independent chronometers, ostensibly owing to the thermal stability of the TT-OSL source trap (Shen et al., 2011; Thiel et al., 2012; Chapot et al., 2016; Faershtein et al., 2018). However, stability of the TT-OSL signal is still debated, with some workers reporting TT-OSL age underestimation beginning near ca. 200 ka (e.g., Thiel et al., 2012) and others finding no age underestimation relative to independent age control even beyond 800 ka (Arnold and Demuro, 2015). Based on the model of Faershtein et al. (2018), the TT-OSL ages reported here for the Buffalo River may be underestimated by 5–10%. Nevertheless, this potential underestimation still falls within our reported age uncertainties and should therefore not have a significant effect on our interpretations. Future work performing pulse annealing experiments would help to determine the thermal lifetime of the TT-OSL traps from quartz along the Buffalo River.

Timescales of terrace occupation

Our results show that terrace ages can be highly variable depending on where in the alluvial fill an OSL sample is collected (Fig. 2). At the three Qtm study sites, samples collected from a single trench yield ages that span ca. 200 ka (Table 1). Similar observations of age variability in terraces have been made using a combination of OSL and cosmogenic nuclide surface exposure dating along Colorado's western High Plains (Foster et al., 2017). Accumulation through overbank and overland flooding apparently can occur over hundreds of thousands of years, which is consistent with the work of Neely (1985) who demonstrated that 100-year floods along the Buffalo River can extend up to 12 m above the normal river level. However, the Qtm terraces studied here apparently do not preserve any sedimentological evidence for discrete episodes of floodplain deposition that would support the variability in ages that we observe. Any interpretations of bedrock incision rates that rely on age data collected from alluvium overlying a strath should be considered with extreme caution. As Pederson et al. (2006) similarly argued, only ages collected near the strath unconformity can truly approximate the timing of strath planation, particularly where terrace fill is thick. In addition, where meandering channels preferentially migrate laterally and terrace elevations are lower, as in the lower resistance Boone Formation (Keen-Zebert et al., 2017), there may be a higher probability for channel reoccupation, reworking, or episodes of renewed aggradation of a strath terrace. We found no evidence for cut-in-fill sequences in our profiles, but that does not preclude the possibility that they exist elsewhere. To avoid erroneous age interpretation, we recommend that sampling strategy be determined only after careful mapping and evaluation of the subsurface has taken place.

Lithologic control on vertical bedrock incision rates

The results presented in this study show that significant differences in vertical bedrock incision rates exist between Buffalo River lithologies that feature variable chemical weathering characteristics. The differences in vertical incision rate closely mirror the differences in terrace tread elevation between lithological reaches; where the river incises the less-resistant Boone Formation reaches, Qtm terrace treads are lower in elevation and OSL-derived incision rates are lower than those obtained from the more-resistant Everton Formation reaches (Fig. 2). The OSL-derived bedrock incision rates presented in this study support the work of Keen-Zebert et al. (2017) who established a relationship between lithology and valley width and terrace distribution along the Buffalo River. Where the river incises the more-resistant Everton Formation, valleys are narrower and preserve a greater number of Qto terraces in the landscape compared to reaches where the channel incises the less-resistant Boone Formation. These characteristics were attributed to variations in the style and rates of vertical versus lateral processes in the different lithologic reaches of the Buffalo River (Keen-Zebert et al., 2017). Our OSL results support these observations and suggest that vertical bedrock incision is statistically higher in the more-resistant Everton Formation reaches relative to the Boone Formation reaches (~35 mm/ka vs. ~16 mm/ka, respectively).

The timescales of vertical versus lateral processes at each of the three study sites are further supported by Zunka (2018) who report lateral migration rates using in-situ produced ^{10}Be concentrations from bluff-derived chert for various locations along the

Buffalo River (see Fig. 1 for sample locations). A relationship between lateral migration rate and changes in bluff lithology was observed; meanders in the Boone Formation reach yielded faster average lateral migration rates relative to those where sandstone units were present (5 mm/ka relative to 109 mm/ka). Even though these rates integrate over shorter timescales relative to the OSL-derived vertical incision rates that we report, together they still support the observations of Keen-Zebert et al. (2017) and suggest that over both shorter and longer timescales the rates of vertical and lateral processes vary as a function of lithologic resistance.

Timescales of channel incision and landscape lowering

Along the Buffalo River, we calculate OSL-derived vertical incision rates for Qtm strath terraces ranging from ~16 mm/ka in the Boone Formation hosted straths to ~35 mm/ka where the channel has incised the Everton Formation. These rates are both faster and slower than previously reported estimates of landscape lowering along the Buffalo River based on different geochronometers. Hudson et al. (2017) used U/Th ages from tufa preserved at Big Bluff ~120 m above the Buffalo River to estimate a maximum incision rate of 740 mm/ka, which is a significantly higher rate than our estimates (Fig. 1).

Previous studies of modern in-channel calcite dissolution rates have been reported as 1.06 mm/yr at Boxley (Boone Formation; Covington et al., 2015), and since revised with the new methodology of Covington and Vaughn (2019) to reflect rates that are likely 30–50% of that value (0.3–0.5 mm/yr or 300–500 mm/ka) (Fig. 1). Even with updated estimates, the calcite dissolution rates are significantly higher than our vertical incision rates of ~16 mm/ka at Margaret White where the channel has incised the Boone Formation limestone. Plausible explanations for the discrepancy include: (a) the modeled dissolution rates assume pure carbonate and may not accurately reflect dissolution of Boone Formation limestone, which is up to 70% chert in some locations (Keen-Zebert et al., 2017); or (b) the primary controllers of dissolution rate (PCO_2 , temperature, and discharge; Covington et al., 2015) have not been constant through time. Moreover, in contrast to modern estimates of in-channel dissolution, OSL-derived incision rates integrate lateral and vertical processes over timescales ranging from thousands to hundreds of thousands of years.

Zunka (2018) reported catchment-averaged denudation rates derived from in-situ produced terrestrial cosmogenic nuclide (^{10}Be) concentrations that range from 16–18 mm/ka (averaged over ca. 35 ka), which are rates that are slightly higher than the estimates of Beeson et al. (2017) who report an average of 8 mm/ka for the broader Ozark Plateaus region. Our calculated vertical bedrock incision rates that average over the last ca. 250 ka are of the same order of magnitude as Zunka's catchment-averaged denudation rates. Zunka (2018) also measured lateral bluff erosion rates from ^{10}Be and used slip-off slope geometry to estimate ratios of lateral to vertical erosion to infer longer term average vertical incision rates of ~2 m/Ma (2 mm/ka). Together with the presence of prominent river bluffs, local catchment averaged denudation rates (Zunka, 2018), and our OSL-derived vertical bedrock incision rates, these results imply that most of the vertical incision along the Buffalo River was completed prior to the last ca. 250 ka.

Most landscape evolution models assume that landscapes evolve through time toward dynamic equilibrium conditions where the rates of hillslope and channel processes are coupled

(e.g., Hack, 1960; Kirkby, 1986; Howard, 1994). However, evidence for transient evolution is not uncommon in natural landscapes (e.g., Beeson et al., 2017; Mudd, 2017). Discrepancies in short term versus long term rates of incision are possible if there are significant hiatuses in channel incision (i.e., the Sadler effect) (Finnegan et al., 2014). This phenomenon could explain both the higher bedrock incision rates captured by OSL, catchment-averaged denudation rates (Zunka 2018), and calcite dissolution (Covington et al., 2015), which average over significantly shorter timescales relative to the vertical incision rate estimates using ^{10}Be and slip-off geometry provided by Zunka (2018). In landscapes with heterogeneous lithology, deviation from steady state conditions may be especially likely because variability in bedrock resistance to erosion can amplify or mitigate topographic responses to forcings (Cook et al., 2009; Forte et al., 2016; DiBiase et al., 2018). Our work builds upon the growing body of literature that suggests that decoupling of hillslope-channel processes over millennial timescales is not uncommon in natural environments.

Controls on the timing of terrace aggradation, incision, and abandonment

A variety of processes may have led to the formation and preservation of the terraces along the Buffalo River. The terraces may indicate local or regional base level change (e.g., Gran et al., 2013) or fluctuations in sediment supply and/or hydrologic conditions driven by climate change (e.g., Wegmann and Pazzaglia, 2002). It is also possible that the terraces formed from autocyclic forces independent of external forcing (Bull, 1990) or from bedrock meandering cutoff dynamics (Finnegan and Dietrich, 2011). In the following section, we discuss the timing of terrace formation along the Buffalo River in the context of known sea level and regional paleoclimatic events.

Our OSL dating results suggest that strath planation was complete by ca. 250 ka, near the Marine Isotope Stage (MIS) 8/MIS 7 boundary (Fig. 6). Strath planation in temperate regions is most commonly associated with periods of increased sediment supply and/or decreases in discharge that most commonly occur during glacial periods (Pazzaglia and Brandon, 2001; Wegmann and Pazzaglia, 2009; García and Mahan, 2014; Schanz et al., 2018). At Fitton Cave within the Buffalo River watershed (Fig. 1), a speleothem record shows decreased growth rates and marked increases in both the $\delta^{13}\text{C}$ and $\delta^{18}\text{O}$ isotopic records between ca. 260–280 ka, possibly indicating a shift to drier conditions during this time (Fig. 6; Paces et al., 2017). There is also some evidence to suggest that even south of the glacial limit, periglacial processes can lead to significant increases in sediment supply during glacial periods, which could allow for a shift to fluvial regimes that favor strath planation (Marshall et al., 2015, 2021).

Strath planation was followed by an extensive aggradational period that apparently persisted through to the last glacial period ca. 35 ka. A gap in the depositional record exists between ca. 220 ka and ca. 120 ka, which is possibly a reflection of sampling bias (Fig. 6). It is also possible that this gap reflects a period of non-deposition or erosion of the sedimentary record, but we find no evidence for buried soil horizons or cut-in-fill activity that would be expected if terraces experienced periods of long-term stability or if they were re-occupied by a younger channel.

Qtm terrace incision and abandonment occurred comparatively rapidly between ca. 35 ka and ca. 11 ka in response to an increase in water discharge, a decrease in sediment supply,

or a drop in base-level (Schanz et al., 2018). The end of Qtm aggradation coincides with the last glacial maximum (LGM) near the transition between MIS 3 and MIS 2 (Fig. 6). Glaciation did not extend as far south as the Buffalo River, but paleoclimate studies in the region suggest that climate transitioned from relatively warm and dry conditions to cool and wet conditions in the transition between MIS 3 and MIS 2. Mineralogic changes in clay sediments deposited in the Gulf of Mexico suggest that moisture inflow into the Midcontinent was reduced during MIS 3 (Sionneau et al., 2013). In contrast, during MIS 2 climates in the Midcontinent were relatively cooler and wetter, as indicated by a shift to C_3 vegetation in Nebraska and Kansas (Johnson and Willey, 2000), by $\delta^{13}\text{C}$ and $\delta^{18}\text{O}$ contents from stalagmites in central Missouri (Dorale et al., 1998), and by rapid speleothem growth in central Texas (Fig. 6D; Musgrove et al., 2001). Terrace incision during MIS 2 also has been reported for the Cimarron River Valley in southwestern Kansas (Fig. 6; Layzell et al., 2015) and Owl Creek, a tributary of the Brazos River in central Texas (Fig. 6; Meier et al., 2013). Base level decrease also could have played a role in driving incision through upward-propagating knickpoints during early MIS 2 when eustatic sea level was ~ 120 m below the present (Fig. 6; Spratt and Lisiecki, 2016). Base level control has been suggested for alluvial terrace incision along the lower Mississippi River, despite their long distance (up to ~ 600 km) from the present-day Gulf of Mexico shoreline (Fig. 6; Shen et al., 2012), but this interpretation has been controversial (see discussion in Otvos, 2013).

The youngest (Qty) terraces preserved along the Buffalo River aggraded during MIS 1 beginning ca. 14.5 ka. The timing of Qty terrace aggradation along the Buffalo River is consistent with aggradational units preserved regionally, including the Brazos (Waters and Nordt, 1995), Owl Creek (Fig. 6H; Meier et al., 2013), and Colorado rivers (Blum and Price, 1998) in central Texas; the Cimarron (Fig. 6; Layzell et al., 2015), Pawnee (Bettis and Mandel, 2002), and Arkansas rivers (Forman et al., 2008) in Kansas; and the Pomme de Terre River in southern Missouri (Brakenridge, 1981). During early MIS 1, the Ozark Plateau was characterized by a shift from cold-adapted boreal forest to mixed conifer-northern hardwoods forest that favors more temperate climates (King, 1973). Between ca. 11–3 ka, the regional climate shifted to warmer, drier, steppe conditions, as evinced by $\delta^{13}\text{C}$ records from stalagmites throughout Missouri and north-central Arkansas (Fig. 6; Denniston et al., 1999, 2000), palynological data from Missouri (Jones et al., 2017; King, 1973), and loess deposition in west-central Kansas (Olson et al., 1997). The regional shift to drier conditions between ca. 11–3 ka is broadly consistent with the timing of Qty aggradation along the Buffalo River. An overall decrease in precipitation could result in reduced river discharge, which would promote terrace aggradation (e.g., Wong et al., 2015). Incision of the Qty terraces likely began in the Middle to Late Holocene, but its precise timing is difficult to determine because high floods likely continue to contribute sediment to terrace treads (Neely, 1985). Over the last ca. 3 ka, climates in the region were characterized by wetter conditions (Delcourt and Delcourt, 1996; Jones et al., 2017), potentially offering a driving mechanism for Qty terrace incision. The synchronicity of regional aggradational events suggests that the timing of terrace aggradation and incision along the Buffalo River likely varies with the timing of regional climatic events, which can influence hydrologic processes and changes in sediment supply.

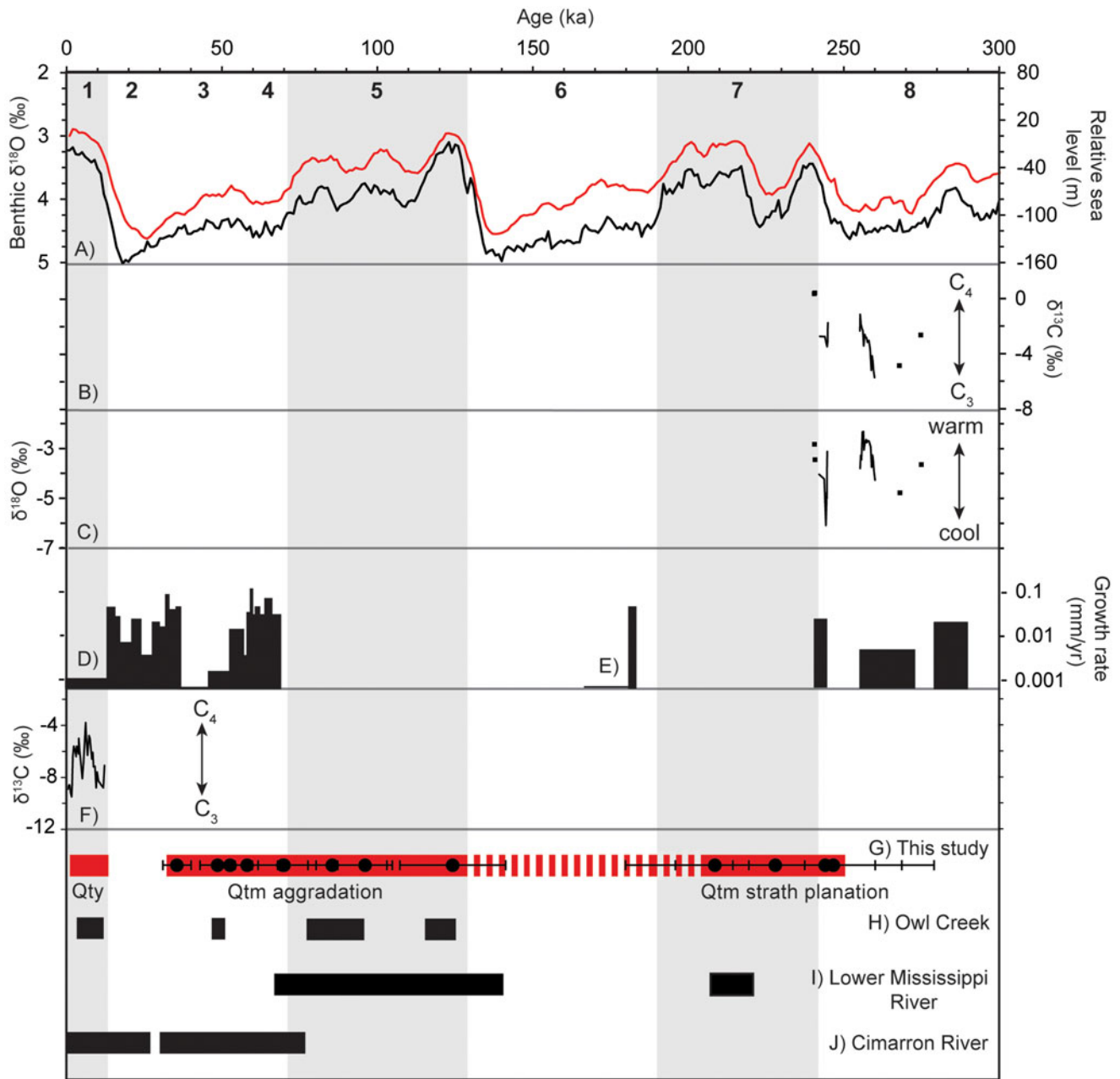


Figure 6. Composite regional paleoenvironmental and fluvial records. Marine Isotope Stages are listed as bold black numbers at the top of the figure. Interglacial stages are shown as vertical gray bands; glacial stages are shown as white bands. Marine isotope substages are not shown here. (A) Fluctuations in benthic $\delta^{18}\text{O}$ composition provided by Lisiecki and Raymo (2005) is shown in black; the relative eustatic sea level reconstruction by Spratt and Lisiecki (2016) is shown in red; (B, C) paired $\delta^{13}\text{C}$ and $\delta^{18}\text{O}$ records from speleothems at Fitton Cave, AR, respectively (Paces *et al.*, 2017); (D) speleothem growth rates from central Texas (Musgrove *et al.*, 2001); (E) speleothem growth rates from Fitton Cave, AR (Paces *et al.*, 2017); (F) $\delta^{13}\text{C}$ records from speleothems at Beckham Creek Cave, AR (Denniston *et al.*, 1999); (G) OSL ages for the Qtm and Qty terraces preserved along the Buffalo River; individual ages with errors for Qtm deposits are shown as circles; individual Qty ages are not shown here (refer to Tables 1 and 2 for a list of OSL ages); (H) ages of terraces preserved along Owl Creek, a tributary of the Brazos River in Central Texas (Meier *et al.*, 2013); (I) ages of Prairie Complex terraces along the lower Mississippi River (Shen *et al.*, 2012); (J) ages of terraces preserved along the Cimarron River in the High Plains of southwestern Kansas (Layzell *et al.*, 2015).

CONCLUSIONS

In this study, we have developed an OSL-based reconstruction of the late Quaternary aggradational and incisional history of the Buffalo River from the alluvium collected from strath and fill terraces. Our TT-OSL ages suggest a minimum planation age of ca. 250 ka for the Qtm terraces and an aggradational phase that apparently persisted for ca. 200 ka. Importantly, our results

from modern analogue samples suggest that the fluvial sediments along the Buffalo River were well bleached at deposition and that a TT-OSL protocol can be used reliably to extend the upper dating limit beyond the range of conventional quartz OSL techniques. Qtm aggradation was punctuated by an incisional period, which likely occurred near the LGM between ca. 35 ka and 11 ka. The onset of Qty terrace aggradation occurred downstream (ca. 14 ka) with a response that propagated upstream

forming the youngest terrace deposits (ca. 5 ka). The long history of Q_{tm} aggradation suggests that terraces along the Buffalo River can continue to aggrade over hundreds of thousands of years. Consequently, interpretations built on assumptions of geologically instantaneous alluvial deposition following strath planation and abandonment should be considered with caution, particularly where thick sequences of alluvial fill are preserved over strath terraces. Our OSL ages suggest that there is some correlation between the timing of Q_{ty} and Q_{tm} terrace aggradation and incision during drier and wetter paleohydrological conditions, respectively.

Our OSL age estimates also suggest that vertical incision rates vary spatially with lithologic resistance along the Buffalo River—where the channel has incised the less-resistant Boone Formation, vertical bedrock incision rates are lower relative to the higher resistance Everton Formation. This work has served to substantiate previous observations relating valley width and lithological resistance along the Buffalo River that have suggested that lateral processes outpace vertical processes in reaches with lower resistance. Lithologic resistance can mitigate or amplify in-channel erosion rates, the effects of which can potentially propagate through an entire catchment. Over the timescales of observation in this study (ca. 250 ka), our in-channel incision rates along the Buffalo River diverge from catchment erosion rates resulting in topography that is characterized by bluffs and wide floodplains.

Supplementary material. The supplementary material for this article can be found at <https://doi.org/10.1017/qua.2023.16>.

Acknowledgments. This research was supported by a National Science Foundation (NSF) grant to Keen-Zebert (EAR 1360572). The work conducted in the Buffalo National River was in compliance with NPS Scientific Research and Collecting Permit #BUFF-2017-SCI-0001, Study #BUFF-00035. The authors thank Harrison Gray, Sarah Schanz, Dong-Eun Kim, and Yeong Bae Seong for their thoughtful and thorough reviews that contributed to the improvement of this manuscript. Any use of trade, firm, or product names is for descriptive purposes only and does not imply endorsement by the U.S. Government.

REFERENCES

- Aitken, M.J., 1998. *Introduction to Optical Dating: The Dating of Quaternary Sediments by the Use of Photon-stimulated Luminescence*. Clarendon Press, Oxford, UK.
- Anthony, D.M., Granger, D.E., 2007. A new chronology for the age of Appalachian erosional surfaces determined by cosmogenic nuclides in cave sediments. *Earth Surface Processes and Landforms* **32**, 874–887.
- Arnold, L.J., Demuro, M., 2015. Insights into TT-OSL signal stability from single-grain analyses of known-age deposits at Atapuerca, Spain. *Quaternary Geochronology* **30**, 472–478.
- Bateman, M.D., Boulter, C.H., Carr, A.S., Frederick, C.D., Peter, D., Wilder, M., 2007. Detecting post-depositional sediment disturbance in sandy deposits using optical luminescence. *Quaternary Geochronology* **2**, 57–64.
- Beeson, H.W., McCoy, S.W., Keen-Zebert, A., 2017. Geometric disequilibrium of river basins produces long-lived transient landscapes. *Earth and Planetary Science Letters* **475**, 34–43.
- Bettis, E.A., III, Mandel, R.D., 2002. The effects of temporal and spatial patterns of Holocene erosion and alluviation on the archaeological record of the Central and Eastern Great Plains, USA. *Geochronology* **17**, 141–154.
- Bishop, P., Goldrick, G., 2010. Lithology and the evolution of bedrock rivers in post-orogenic settings: constraints from the high-elevation passive continental margin of SE Australia. *Geological Society, London, Special Publications* **346**, 267–287.
- Blum, M.D., Price, D.M., 1998. Quaternary Alluvial Plain Construction in Response to Glacio-Eustatic and Climatic Controls, Texas Gulf Coastal Plain. In: Kocurek, G. (Ed.), *Relative Role of Eustasy, Climate, and Tectonism in Continental Rocks*. SEPM (Society for Sedimentary Geology). <https://doi.org/10.2110/pec.98.59.0031>.
- Brakenridge, G.R., 1981. Late Quaternary floodplain sedimentation along the Pomme de Terre River, southern Missouri. *Quaternary Research* **15**, 62–76.
- Bufe, A., Paola, C., Burbank, D.W., 2016. Fluvial bevelling of topography controlled by lateral channel mobility and uplift rate. *Nature Geoscience* **9**, 706–710.
- Bull, W.B., 1990. Stream-terrace genesis: implications for soil development. *Geomorphology* **3**, 351–367.
- Bull, W.B., 1991. *Geomorphic Responses to Climatic Change*. Oxford University Press, Oxford, UK.
- Chandler, A.K., Ausbrooks, S.M., 2015a. Geologic map of the Mt. Judea quadrangle, Newton County, Arkansas. *Arkansas Geological Survey Digital Geologic Quadrangle Map DGM-AR-00590*, 1:24,000 scale. https://www.geology.arkansas.gov/docs/pdf/maps-and-data/geologic_maps/24k/Mount%20Judea.pdf.
- Chandler, A.K., Ausbrooks, S.M., 2015b. Geologic map of the Snowball quadrangle, Searcy County, Arkansas. *Arkansas Geological Survey Digital Geologic Quadrangle Map DGM-AR-00800*, 1:24,000 scale. https://www.geology.arkansas.gov/docs/pdf/maps-and-data/geologic_maps/24k/Snowball.pdf.
- Chapot, M., Roberts, H., Duller, G., Lai, Z., 2016. Natural and laboratory TT-OSL dose response curves: testing the lifetime of the TT-OSL signal in nature. *Radiation Measurements* **85**, 41–50.
- Cook, K.L., Whipple, K.X., Heimsath, A.M., Hanks, T.C., 2009. Rapid incision of the Colorado River in Glen Canyon—insights from channel profiles, local incision rates, and modeling of lithologic controls. *Earth Surface Processes and Landforms* **34**, 994–1010.
- Covington, M.D., Gulley, J.D., Gabrovšek, F., 2015. Natural variations in calcite dissolution rates in streams: controls, implications, and open questions. *Geophysical Research Letters* **42**, 2836–2843.
- Covington, M.D., Vaughn, K.A., 2019. Carbon dioxide and dissolution rate dynamics within a karst underflow-overflow system, Savoy Experimental Watershed, Arkansas, USA. *Chemical Geology* **527**, 118689. <https://doi.org/10.1016/j.chemgeo.2018.03.009>.
- Croneis, C., 1930. Geology of the Arkansas Paleozoic area, with especial reference to oil and gas possibilities. *Arkansas Geological Survey Bulletin* **3**, 1–457.
- Delcourt, P.A., Delcourt, H.R., 1996. Quaternary paleoecology of the Lower Mississippi Valley. *Engineering Geology* **45**, 219–242.
- Demuro, M., Arnold, L.J., Parés, J.M., Sala, R., 2015. Extended-range luminescence chronologies suggest potentially complex bone accumulation histories at the Early-to-Middle Pleistocene palaeontological site of Huéscar-1 (Guadix-Baza basin, Spain). *Quaternary International* **389**, 191–212.
- Denniston, R.F., González, L.A., Asmerom, Y., Reagan, M.K., Recelli-Snyder, H., 2000. Speleothem carbon isotopic records of Holocene environments in the Ozark Highlands, USA. *Quaternary International* **67**, 21–27.
- Denniston, R.F., Gonzalez, L.A., Semken, H.A., Asmerom, Y., Baker, R.G., Recelli-Snyder, H., Reagan, M.K., Bettis, E.A., 1999. Integrating stalagmite, vertebrate, and pollen sequences to investigate Holocene vegetation and climate change in the southern Midwestern United States. *Quaternary Research* **52**, 381–387.
- DiBiase, R.A., Denn, A.R., Bierman, P.R., Kirby, E., West, N., Hidy, A.J., 2018. Stratigraphic control of landscape response to base-level fall, Young Womans Creek, Pennsylvania, USA. *Earth and Planetary Science Letters* **504**, 163–173.
- Dorale, J.A., Edwards, R.L., Ito, E., González, L.A., 1998. Climate and vegetation history of the Midcontinent from 75 to 25 ka: a speleothem record from Crevice Cave, Missouri, USA. *Science* **282**, 1871–1874.
- Duller, G.A.T., 2003. Distinguishing quartz and feldspar in single grain luminescence measurements. *Radiation Measurements* **37**, 161–165.
- Duller, G., Wintle, A., 2012. A review of the thermally transferred optically stimulated luminescence signal from quartz for dating sediments. *Quaternary Geochronology* **7**, 6–20.
- Faershtein, G., Guralnik, B., Lambert, R., Matmon, A., Porat, N., 2018. Investigating the thermal stability of TT-OSL main source trap. *Radiation Measurements* **119**, 102–111.

- Finnegan, N.J., Dietrich, W.E., 2011. Episodic bedrock strath terrace formation due to meander migration and cutoff. *Geology* **39**, 143–146.
- Finnegan, N.J., Schumer, R., Finnegan, S., 2014. A signature of transience in bedrock river incision rates over timescales of 104–107 years. *Nature* **505**, 391–394.
- Forman, S.L., Marín, L., Gomez, J., Pierson, J., 2008. Late Quaternary eolian sand depositional record for southwestern Kansas: landscape sensitivity to droughts. *Palaeogeography, Palaeoclimatology, Palaeoecology* **265**, 107–120.
- Forte, A.M., Yanites, B.J., Whipple, K.X., 2016. Complexities of landscape evolution during incision through layered stratigraphy with contrasts in rock strength. *Earth Surface Processes and Landforms* **41**, 1736–1757.
- Foster, M.A., Anderson, R.S., Gray, H.J., Mahan, S.A., 2017. Dating of river terraces along Lefthand Creek, western High Plains, Colorado, reveals punctuated incision. *Geomorphology* **295**, 176–190.
- Galbraith, R.F., Roberts, R.G., Laslett, G.M., Yoshida, H., Olley, J.M., 1999. Optical dating of single and multiple grains of quartz from Jinmium Rock Shelter, Northern Australia: part I, experimental design and statistical models. *Archaeometry* **41**, 339–364.
- García, A.F., Mahan, S.A., 2014. The notion of climate-driven strath-terrace production assessed via dissimilar stream-process response to late Quaternary climate. *Geomorphology* **214**, 223–244.
- Gilbert, G.K., 1877. *Geology of the Henry Mountains*. US Geological and Geographical Survey of the Rocky Mountain Region, Government Printing Office, Washington, D.C. <https://doi.org/10.3133/70038096>.
- Gran, K.B., Finnegan, N., Johnson, A.L., Belmont, P., Wittkop, C., Rittenour, T., 2013. Landscape evolution, valley excavation, and terrace development following abrupt postglacial base-level fall. *Geological Society of America Bulletin* **125**, 1851–1864.
- Guérin, G., Christophe, C., Philippe, A., Murray, A.S., Thomsen, K.J., Tribolo, C., Urbanová, P., Jain, M., Guibert, P., Mercier, N., 2017. Absorbed dose, equivalent dose, measured dose rates, and implications for OSL age estimates: introducing the Average Dose Model. *Quaternary Geochronology* **41**, 163–173.
- Guérin, G., Mercier, N., Adamiec, G., 2011. Dose-rate conversion factors: update. *Ancient TL* **29**, 5–8.
- Hack, J.T., 1960. Interpretation of erosional topography in humid temperate regions. *American Journal of Science* **258**, 80–97.
- Hancock, G.S., Anderson, R.S., 2002. Numerical modeling of fluvial strath-terrace formation in response to oscillating climate. *Geological Society of America Bulletin* **114**, 1131–1142.
- Harkins, N.W., Anastasio, D.J., Pazzaglia, F.J., 2005. Tectonic geomorphology of the Red Rock fault, insights into segmentation and landscape evolution of a developing range front normal fault. *Journal of Structural Geology* **27**, 1925–1939.
- Howard, A.D., 1994. A detachment-limited model of drainage basin evolution. *Water Resources Research* **30**, 2261–2285.
- Hudson, M.R., Paces, J.B., Turner, K.J., 2017. Tufa and water radiogenic geochemistry and tufa ages for two karst aquifers in the Buffalo National River region, northern Arkansas. In: Kuniansky, E.L., Spangler, L.E. (Eds.), *US Geological Survey Karst Interest Group Proceedings, San Antonio, Texas, May 16–18, 2017. Scientific Investigations Report 2017-5023*, 107–118.
- Hudson, M.R., Turner, K.J., 2022. Late Paleozoic flexural extension and overprinting shortening in the southern Ozark dome, Arkansas, USA: evolving fault kinematics in the foreland of the Ouachita orogen. *Tectonics* **41**, e2021TC006706. <https://doi.org/10.1029/2021TC006706>.
- Hudson, M.R., Turner, K.J., Bitting, C., 2011. Geology and karst landscapes of the Buffalo National River area, northern Arkansas. In: Kuniansky, E.L., U.S. Geological Survey Karst Interest Group Proceedings, Fayetteville, Arkansas, April 26–29, 2011. *U.S. Geological Survey Scientific Investigations Report 2011-5031*, 191–212.
- Hu, G., Zhang, J.-F., Qiu, W.-L., Zhou, L.-P., 2010. Residual OSL signals in modern fluvial sediments from the Yellow River (HuangHe) and the implications for dating young sediments. *Quaternary Geochronology* **5**, 187–193.
- Jain, M., Murray, A.S., Botter-Jensen, L., 2004. Optically stimulated luminescence dating: how significant is incomplete light exposure in fluvial environments? *Quaternaire* **15**, 143–157.
- Johnson, W.C., Willey, K.L., 2000. Isotopic and rock magnetic expression of environmental change at the Pleistocene–Holocene transition in the central Great Plains. *Quaternary International* **67**, 89–106.
- Jones, R.A., Williams, J.W., Jackson, S.T., 2017. Vegetation history since the last glacial maximum in the Ozark highlands (USA): a new record from Cupola Pond, Missouri. *Quaternary Science Reviews* **170**, 174–187.
- Keen-Zebert, A., Hudson, M.R., Shepherd, S.L., Thaler, E.A., 2017. The effect of lithology on valley width, terrace distribution, and bedload provenance in a tectonically stable catchment with flat-lying stratigraphy. *Earth Surface Processes and Landforms* **42**, 1573–1587.
- King, J.E., 1973. Late Pleistocene palynology and biogeography of the Western Missouri Ozarks. *Ecological Monographs* **43**, 539–565.
- Kirkby, M.J., 1986. A two dimensional simulation model for slope and stream evolution. In: Abrahams, A.D. (Ed.), *Hillslope Processes, Binghamton Geomorphology Symposium 16*. Allen and Unwin, Winchester, MA, pp. 203–222.
- Lavé, J., Avouac, J.P., 2001. Fluvial incision and tectonic uplift across the Himalayas of central Nepal. *Journal of Geophysical Research: Solid Earth* **106**, 26561–26591.
- Layzell, A.L., Mandel, R.D., Ludvigson, G.A., Rittenour, T.M., Smith, J.J., 2015. Forces driving Late Pleistocene (ca. 77–12 ka) landscape evolution in the Cimarron River valley, southwestern Kansas. *Quaternary Research* **84**, 106–117.
- Limaye, A.B.S., Lamb, M.P., 2014. Numerical simulations of bedrock valley evolution by meandering rivers with variable bank material. *Journal of Geophysical Research: Earth Surface* **119**, 927–950.
- Limaye, A.B.S., Lamb, M.P., 2016. Numerical model predictions of autogenic fluvial terraces and comparison to climate change expectations. *Journal of Geophysical Research: Earth Surface* **121**, 512–544.
- Liritzis, I., Stamoulis, K., Papachristodoulou, C., Ioannides, K., 2013. A re-evaluation of radiation dose-rate conversion factors. *Mediterranean Archaeology and Archaeometry* **13**(3), 1–15.
- Lisiecki, L.E., Raymo, M.E., 2005. A Pliocene–Pleistocene stack of 57 globally distributed benthic $\delta^{18}\text{O}$ records. *Paleoceanography* **20**, PA1003. <https://doi.org/10.1029/2004PA001071>.
- Marcotte, A.L., Neudorf, C.M., Langston, A.L., 2021. Lateral bedrock erosion and valley formation in a heterogeneously layered landscape, northeast Kansas. *Earth Surface Processes and Landforms* **46**, 2248–2263.
- Marshall, J.A., Roering, J.J., Bartlein, P.J., Gavin, D.G., Granger, D.E., Rempel, A.W., Praskievicz, S.J., Hales, T.C., 2015. Frost for the trees: did climate increase erosion in unglaciated landscapes during the late Pleistocene? *Science Advances* **1**, e1500715. <https://doi.org/10.1126/sciadv.1500715>.
- Marshall, J.A., Roering, J.J., Rempel, A.W., Shafer, S.L., Bartlein, P.J., 2021. Extensive frost weathering across unglaciated North America during the last glacial maximum. *Geophysical Research Letters* **48**, e2020GL090305. <https://doi.org/10.1029/2020GL090305>.
- Meier, H.A., Nordt, L.C., Forman, S.L., Driese, S.G., 2013. Late Quaternary alluvial history of the middle Owl Creek drainage basin in central Texas: a record of geomorphic response to environmental change. *Quaternary International* **306**, 24–41.
- Merritts, D.J., Vincent, K.R., Wohl, E.E., 1994. Long river profiles, tectonism, and eustasy: a guide to interpreting fluvial terraces. *Journal of Geophysical Research: Solid Earth* **99**, 14031–14050.
- Montgomery, D.R., 2004. Observations on the role of lithology in strath terrace formation and bedrock channel width. *American Journal of Science* **304**, 454–476.
- Mott, D., Luraas, J., 2004. *Buffalo National River, Arkansas Water Resources Management Plan*. National Park Service, U.S. Department of the Interior, Washington, DC, 144 pp.
- Mudd, S.M., 2017. Detection of transience in eroding landscapes. *Earth Surface Processes and Landforms* **42**, 24–41.
- Murray, A.S., Wintle, A.G., 2000. Luminescence dating of quartz using an improved single-aliquot regenerative-dose protocol. *Radiation Measurements* **32**, 57–73.
- Murray, A.S., Wintle, A.G., 2003. The single aliquot regenerative dose protocol: potential for improvements in reliability. *Radiation Measurements* **37**, 377–381. [https://doi.org/10.1016/S1350-4487\(03\)00053-2](https://doi.org/10.1016/S1350-4487(03)00053-2).

- Musgrove, M., Banner, J.L., Mack, L.E., Combs, D.M., James, E.W., Cheng, H., Edwards, R.L., 2001. Geochronology of Late Pleistocene to Holocene speleothems from central Texas: implications for regional paleoclimate. *Geological Society of America Bulletin* **113**, 1532–1543.
- Neely, B.L., 1985. The flood of December 1982 and the 100- and 500-year flood on the Buffalo River, Arkansas. *US Geological Survey, Water-Resources Investigations Report* 85–4192. <https://doi.org/10.3133/wri854192>.
- Olley, J.M., Pietsch, T., Roberts, R.G., 2004. Optical dating of Holocene sediments from a variety of geomorphic settings using single grains of quartz. *Geomorphology* **60**, 337–358.
- Olson, C., Nettleton, W., Porter, D., Brasher, B., 1997. Middle Holocene aeolian activity on the High Plains of west-central Kansas. *The Holocene* **7**, 255–261.
- Otvos, E.G., 2013. Rapid and widespread response of the Lower Mississippi River to eustatic forcing during the last glacial-interglacial cycle: discussion. *Geological Society of American Bulletin* **125**, 1369–1374.
- Paces, J.B., Hudson, M.R., Hudson, A.M., Turner, K.J., Bitting, C.J., Center, D., 2017. Isotopic Constraints on Middle Pleistocene Cave Evolution, Paleohydrologic Flow, and Environmental Conditions From Fitton Cave Speleothems, Buffalo National River, Arkansas. In: Kuniansky, E.L., Spangler, L.E. (Eds.), *US Geological Survey Karst Interest Group Proceedings, San Antonio, Texas, May 16–18, 2017. Scientific Investigations Report* 2017–5023, 119–132.
- Pazzaglia, F.J., Brandon, M.T., 2001. A fluvial record of long-term steady-state uplift and erosion across the Cascadia forearc high, western Washington State. *American Journal of Science* **301**, 385–431.
- Pederson, J.L., Anders, M.D., Rittenhour, T.M., Sharp, W.D., Gosse, J.C., Karlstrom, K.E., 2006. Using fill terraces to understand incision rates and evolution of the Colorado River in eastern Grand Canyon, Arizona. *Journal of Geophysical Research: Earth Surface* **111**, F02003. <https://doi.org/10.1029/2004JF000201>.
- Personius, S.F., Kelsey, H.M., Grabau, P.C., 1993. Evidence for regional stream aggradation in the Central Oregon Coast Range during the Pleistocene-Holocene transition. *Quaternary Research* **40**, 297–308.
- Porat, N., Duller, G., Roberts, H., Wintle, A., 2009. A simplified SAR protocol for TT-OSL. *Radiation Measurements* **44**, 538–542.
- Prescott, J.R., Hutton, J.T., 1994. Cosmic ray contributions to dose rates for luminescence and ESR dating: large depths and long-term time variations. *Radiation Measurements* **23**, 497–500.
- Rink, W.J., Odom, A.L., 1991. Natural alpha recoil particle radiation and ionizing radiation sensitivities in quartz detected with EPR: implications for geochronometry. *International Journal of Radiation Applications and Instrumentation. Part D. Nuclear Tracks and Radiation Measurements* **18**, 163–173.
- Schanz, S.A., Montgomery, D.R., 2016. Lithologic controls on valley width and strath terrace formation. *Geomorphology* **258**, 58–68.
- Schanz, S.A., Montgomery, D.R., Collins, B.D., Duvall, A.R., 2018. Multiple paths to straths: a review and reassessment of terrace genesis. *Geomorphology* **312**, 12–23.
- Scheingross, J.S., Limaye, A.B., McCoy, S.W., Whittaker, A.C., 2020. The shaping of erosional landscapes by internal dynamics. *Nature Reviews Earth & Environment* **1**, 661–676.
- Shen, Z., Mauz, B., Lang, A., 2011. Source-trap characterization of thermally transferred OSL in quartz. *Journal of Physics D: Applied Physics* **44**, 295405. <https://doi.org/10.1088/0022-3727/44/29/295405>.
- Shen, Z., Tornqvist, T.E., Autin, W.J., Mateo, Z.R.P., Straub, K.M., Mauz, B., 2012. Rapid and widespread response of the Lower Mississippi River to eustatic forcing during the last glacial-interglacial cycle. *Geological Society of America Bulletin* **124**, 690–704.
- Sionneau, T., Bout-Roumazeilles, V., Meunier, G., Kissel, C., Flower, B.P., Bory, A., Tribouillard, N., 2013. Atmospheric re-organization during Marine Isotope Stage 3 over the North American continent: sedimentological and mineralogical evidence from the Gulf of Mexico. *Quaternary Science Reviews* **81**, 62–73.
- Spratt, R.M., Lisiecki, L.E., 2016. A Late Pleistocene sea level stack. *Climate of the Past* **12**, 1079–1092.
- Thiel, C., Buylaert, J.-P., Murray, A.S., Elmejdoub, N., Jedoui, Y., 2012. A comparison of TT-OSL and post-IR IRSL dating of coastal deposits on Cap Bon peninsula, north-eastern Tunisia. *Quaternary Geochronology* **10**, 209–217.
- Turner, K.J., Hudson, M.R., 2010. Geologic map of the Maumee quadrangle, Marion and Searcy Counties, Arkansas. *U.S. Geological Survey Scientific Investigations Map* **3134**, 1:24,000 scale.
- Van Der Woerd, J., Xu, X., Li, H., Tapponnier, P., Meyer, B., Ryerson, F.J., Meriaux, A.-S., Xu, Z., 2001. Rapid active thrusting along the northwestern range front of the Tanghe Nan Shan (western Gansu, China). *Journal of Geophysical Research: Solid Earth* **106**, 30475–30504.
- Wang, X., Lu, Y., Wintle, A., 2006. Recuprated OSL dating of fine-grained quartz in Chinese loess. *Quaternary Geochronology* **1**, 89–100.
- Waters, M.R., Nordt, L.C., 1995. Late Quaternary floodplain history of the Brazos River in east-central Texas. *Quaternary Research* **43**, 311–319.
- Wegmann, K.W., Pazzaglia, F.J., 2002. Holocene strath terraces, climate change, and active tectonics: the Clearwater River basin, Olympic Peninsula, Washington State. *Geological Society of America Bulletin* **114**, 731–744.
- Wegmann, K.W., Pazzaglia, F.J., 2009. Late Quaternary fluvial terraces of the Romagna and Marche Apennines, Italy: climatic, lithologic, and tectonic controls on terrace genesis in an active orogen. *Quaternary Science Reviews* **28**, 137–165. <https://doi.org/10.1016/j.quascirev.2008.10.006>.
- Whipple, K.X., Tucker, G.E., 1999. Dynamics of the stream-power river incision model: implications for height limits of mountain ranges, landscape response timescales, and research needs. *Journal of Geophysical Research: Solid Earth* **104**, 17661–17674.
- Wintle, A.G., Murray, A.S., 2006. A review of quartz optically stimulated luminescence characteristics and their relevance in single-aliquot regeneration dating protocols. *Radiation Measurements* **41**, 369–391.
- Wong, C.I., Banner, J.L., Musgrove, M., 2015. Holocene climate variability in Texas, USA: an integration of existing paleoclimate data and modeling with a new, high-resolution speleothem record. *Quaternary Science Reviews* **127**, 155–173.
- Zunka, J.P.P., 2018. *Controls on Process and Form in Alluvial and Bedrock Meandering Rivers*. PhD dissertation, Oregon State University, Corvallis, OR.